NUMERICAL MODELING AND DESIGN OF SLAB TRACKS

Comparison with ballasted tracks

Samuel Matias[1]

[1]Instituto Superior Técnico, University of Lisbon
Av. Rovisco Pais, 1049-001, Lisboa, Portugal

Keywords: Railway infrastructure, slab track, stedef, ballasted track, finite element modeling, structural design.

Abstract: The increase in velocity and daily circulation of high-speed services results in an extra need for maintenance in the traditional ballasted track which exhibits a pronounced degradation, therefore motivating the investigation of alternative solutions.

It is in this context that several slab track solutions arise, optimized to ensure a high structural stability and reduced maintenance. Thus, the main scope of this paper is to predict the structural behavior for slab track design purposes with special focus on the configurations present in the Chauconin case study located in the French high-speed line LGV- Est (Stedef™ system). Three-dimensional finite element models are developed with proper validation through experimental campaigns conducted by SNCF. With these models, a static comparison is performed between the Stedef™ slab track and the ballasted track, as well as a parametric study to various parameters of the slab track in order to optimize its design. A structural behavior comparison between the Stedef™, Rheda 2000™ and Bögl™ slab tracks is performed, and their response to platform longitudinal stiffness variations is evaluated.

1. Introduction

With the growing velocity of high-speed trains, already established at 350 km/h in some new high-speed lines and tending to increase, a prominent degradation of geometry quality in ballasted tracks was evidenced. This led to an extensive experience and scientific research invested in the deterioration processes of ballasted tracks and its dynamic behavior. However with the current scenario of maintenance needs and availability in high-speed lines, the slab track becomes a alternative and competitive solution whose understanding of its structural behavior, as well as its construction and maintenance, is still expanding.

In order to assess the quality criteria and design of the railway track (ballasted track and slab track), three-dimensional finite element models are those best fitted to its mathematical modeling.

There have been several finite element models developed for the purpose of optimizing the design of the railway track, especially the ballasted solution. Some of these models have been preceded by other programs with more computation power.

In 1976, López Pita was one of the first authors to develop a two-dimensional model of the cross section of the track, being followed by the Illitrack model performed by Robnett Knoston *et. al* (1976-1979) that complements two-dimensional models in order to create a three-dimensional

[1] e-mail: samuel.matias@ist.utl.pt

interpretation of the track. Since then, several nonlinear three-dimensional models have been developed and some of the principal authors are Chang *et. al* (1980), Huang *et. al* (1981) and Profillidis (1983-1987). A better review of the described models can be found in [1]. More recently, models with granular nonlinear behavior and contact elements under the sleeper by Areias [2] and Ferreira *et. al.* [3] were created for the purpose of design optimization through stiffer sub-layers.

Regarding the modeling improvements in slab track, these only appeared more recently with Markine and Esveld [4], who performed studies in the vibration behavior and design optimization of slab tracks with embedded rails with de model "Rail" developed at Delft University. Later, other models were created such as the ones made by Blanco-Lorenzo *et. al* [5] , Vale *et. al* [6] and Poveda *et. al* [7]. The vast majority of the models developed have the objective of studying the dynamic behavior and wave propagation, other than its direct effects on slab track design.

In this scope, the main objective of this paper is to develop a numerical tool that, after being properly validated and tested, enables the estimation of the static response of a slab track system (Stedef^{TM}) with the purpose of optimizing its structural design behaviour.

2. Railway Numerical Modeling

This section introduces the methodology of railway modeling development (in this case, only the ballasted track) and perform a parametric study to the element type used and the model domain. The numerical modeling will be performed using the software ANSYS^{TM} [8].

2.1. Element modeling, domain and boundary conditions

To study the influence of the element type being used, 5 three-dimensional models, which all differ amongst themselves through the rail geometry and element type and the railpad element type (see Table 2.1), will be discussed.

For the rail modeling, the model 3D 1 uses a uniaxial three-dimensional beam element with two nodes (BEAM4) with tensile, compression, bending and torsion behavior. The element has six degrees of freedom at each node: translations in x, y and z and rotations in x, y and z. The models 3D 2 and 3D 3 uses a Timoshenko beam with 2 nodes and the same six degrees of freedom (BEAM188). The railpad in models 3D 1, 3D 2 and 3D 3 is modeled by a spring-damper element with two nodes (COMBIN14) that behaves in uniaxial tension-compression with three degrees of freedom at each node: translations in x, y and z.

Finally, models 3D 4 and 3D 5, the sleepers and the multilayer system of the remaining models use a three-dimensional solid element (SOLID95) defined by 20 nodes with three degrees of freedom per node, translations in x, y and z.

Table 2.1: Designation of the three-dimensional models

Model	Rail element	Pad element
3D 1	3D uniaxial beam	Spring-damper
3D 2	Timoshenko beam (□ section)	
3D 3	Timoshenko beam (I section)	
3D 4	Solid (□ section)	Solid
3D 5	Solid (I section)	

The geometry adopted for the models (3D 2, 3, 4 and 5) that use rail sections are squared (□) and in I shape. In both sections, the width of the flange (base) and the highest inertia (I_y) are equivalent to the UIC60 rail, which are the most important aspects for modeling the first elastic level (see Figure 2.1)

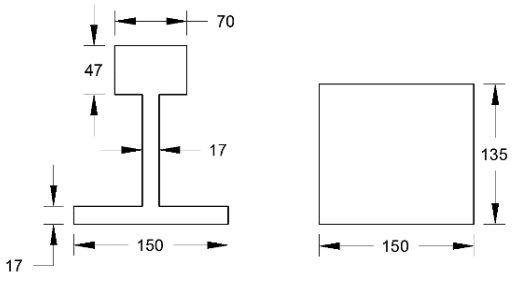

Figure 2.1: Rail section type (units in mm)

In order to take into account the vertical stiffness of the railpad K_p (kN/mm) in solid elements, the equivalent modulus of elasticity is corrected for the actual geometry of the railpad and its Poisson effect through equation (2.1).

$$E_p = K_p \times \frac{h}{l \times c} \frac{(1+\upsilon)(1-2\upsilon)}{(1-\upsilon)} \qquad \textbf{(2.1)}$$

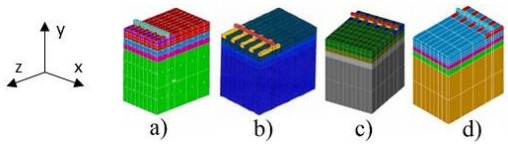

Figure 2.2: 3D FEM developed by Areias (2007) (a), Ministerio de Fomento (1999) (b), Morais (2008) (c) and proposed model 3D 4 (d)

With the purpose of validating the three-dimensional models previously discussed, models already undertaken by Areias [2] and Morais [9] will be recreated, which in turn were validated by the model developed by Ministerio de Fomento [10].

The principal mechanical and geometric element properties of the different models and their domain properties are outlined in Table 2.2:

Table 2.2: Railway Model Properties

Element	E (MPa)	υ (-)	Geometry (yy×zz×xx)
Rail	205800	0.3	□ and I section
Railpad	(244 kN/mm)	0.35	0.135×0.15×0.27
Sleeper	49000	0.25	0.22×2.6×0.27
Ballast	127.4	0.2	0.3×7.4×5.07
Sub-ballast	117.6	0.2	0.3×7.4×5.07
Form layer	19.6	0.3	0.35×7.4×5.07
Platform	5.88	0.35	3×7.4×5.07

The main differences between the models are the use of a non-linear material model for granular materials (Drucker-Prager failure criterion) and the use of contact elements under the sleepers by the model developed by Ministerio de Fomento. For further detail about the models, see [2], [9] and [10].

Taking advantage of the symmetry in the z and x axis of the track, it will only be represented one quarter of the model with symmetry conditions in the respective planes. The boundary conditions applied in the remaining surfaces are the displacement restriction in the orthogonal direction of the surface considered.

2.2. Results

With the aim to investigate the influence of the element type in the behavior of the railway ballasted track the values of vertical displacements of the rail and vertical stress on the top of platform between the several models developed (3D 1-5) will be estimated and compared with the models present in the literature review. To complement the parametric study, 3 variants of each one of the models will be considered, in which the reference model uses a 30 cm sub-ballast layer (S30), and the remaining variants have 15 cm (S15) and 0 cm (S00).

The results of the built models and the models present in the literature are presented in Table 2.3 and Table 2.4.

Table 2.3: Results from the literature review models

		δ (mm)	$\sigma_{plat.}$ (kPa)
MF (1999)	**S30**	3.86	-9.3
	S15	4.13	-10.4
	S00	4.34	-14.0
Areias (2007)	**S30**	2.75	-7.7
	S15	3.15	-9.1
	S00	3.43	-10.2
Morais (2008)	**S30**	2.75	-7.7
	S15	2.99	-8.7
	S00	3.30	-10.1

Table 2.4: 3D 1-5 models results

		3D 1	3D 2	3D 3	3D 4	3D 5
δ (mm)	**S30**	3.20	3.04	2.85	2.94	3.00
	S15	3.50	3.30	3.17	3.16	3.22
	S00	3.89	3.62	3.55	3.44	3.50
$\sigma_{plat.}$ (kPa)	**S30**	-9.23	-8.9	-9.2	-8.1	-8.5
	S15	-10.5	-9.9	-10.4	-9.0	-9.5
	S00	-12.3	-11.3	-12.7	-10.4	-10.7

The results obtained show good theoretical consistency, which makes it possible to draw the following conclusions:

- A three-dimensional uniaxial beam model for the rail (3D 1) shows greater flexibility than the remaining models, which indicates a non-suitable tool for design purposes. Thus, the Timoshenko beam theory and a solid section are a good solution for rail modeling for flexibility evaluation.
- The use of a spring-damper element for railpad modeling overestimates the vertical stress on layer interfaces due to the punctual nature of the load transmission.

Taking this into account, the rail and railpad modeling using solid elements (3D 4-5) are the best approximation to a detailed static modeling of the railway track for design purposes.

For the full development of three-dimensional models, the calibration of the domain proves to be a very important aspect to consider, since its dimension is obtained through an iterative process to evaluate the influence of boundary conditions on the results. The domain of the model is influenced by the stiffness of its components, the geometry of the superstructure and the loading and boundary conditions. Another important aspect is the size of the mesh used, which depends on the

structural response parameter intended to estimate.
The improvement of the ballasted track model implies the inclusion of contact elements under the sleepers, which is an important feature in the degradation of the load, resulting in stress and displacements increase around 20%.

3. Application to LGV-Est Case Study

In this section, several numerical models will be modeled, which are representative of the railway solutions present in Chauconin test section in LGV-Est. This test section consists in two transition zones between ballasted track and slab track (Figure 3.1) where an experimental campaign conducted by SNCF was carried out and performance measurements were collected with the circulation of real trains (TGV Réseau UM and MS).
These experimental in situ measurements are crucial for the proper validation of numerical models to be developed.

3.1. Track and Train Characterization

Figure 3.1: Experimental site [11]

The ballasted track (VB) is composed by UIC60 rails, elastic railpads (180x148x9mm^3), Pandrol Fastclip^{TM} fastening system, Sateba^{TM} D450 monoblock sleepers, a ballast layer (31 cm) and a sub-ballast layer (20 cm). With respect to the ZT1 ballasted track (VBZT1) (present in transition zone 1) it differs from the track previously described, by the inclusion of a ballast mat with 30 mm under a layer of ballast (21.7 cm) and the replacement of sub-ballast by a hydraulic bonded layer with 28 cm (HBL).
The slab track used in this test section (VSB) is the Stedef^{TM} system. In short, the essential features of this system are the two levels of elastic adjustment, ease replacing sleepers and biphased concrete cast.
The system uses a bi-block sleeper (Sateba^{TM} D453 IP), surrounded by a hull elastomer which contains an under sleeper pad (USP) (656×228×12 mm^3) at the bottom, and lateral pads, which provide a flexible joint between the hull and the sleeper. The hull elastomer lies embedded in an upper concrete structure that fills the previously trough-shaped lower structure.
The first stage is the casting of a C35/45 which acts as a container for the casting of the second stage that uses a C30/37 reinforced with polypropylene fibers. At last, all the system rests on a HBL (28 cm).
The rolling stock in operation on LGV-Est and circulating in the test section are TGV-Réseau (SNCF) and ICE (DB). However the recorded measurements are only those corresponding to the TGV-Réseau circulations, whose static axle load is 164.7 kN.

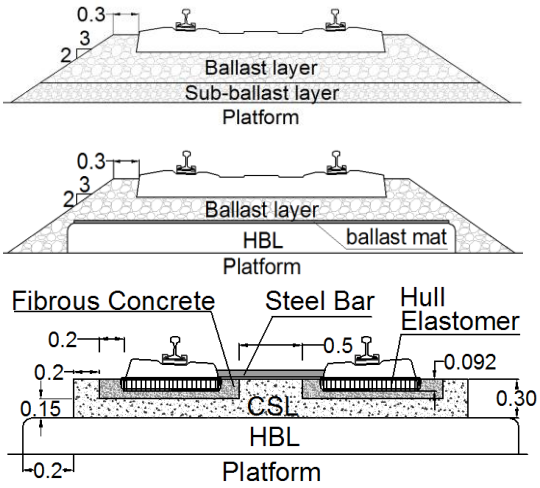

Figure 3.2: Schematic representation of VB (above), VBZT1 (center) and VSB (below) (units in m) (adapted from [11])

3.2. Numerical Modeling

The numerical modeling of the different elements of the respective railway types present in Chauconin test section was performed according to the geometric and mechanical characteristics recorded in the bibliography provided by the Department of Railway Study from Technical Direction of SNCF, as well as the conclusions regarding the development of a railway numerical model taken from the previous section. Therefore, and taking into account the properties of the respective railway tracks present in the case study, each element modeling is carried out as outlined in Figure 3.2. and Table 3.1.

Table 3.1: Properties of Chauconin test section models [13]

Element	Model	E (MPa)	K_p (kN/mm)	K_{bm} (N/mm^3)	υ (-)	ρ (kg/m^3)
Rail	VB/ VBZT1/ VSB	205 800	-	-	0.3	7872
Railpad	VB/ VBZT1/ VSB	-	90/ 120[2]	-	0.25	900
USP	VSB	-	21/ 35[2]	-	0.25	900
Sleepers	VB/ VBZT1	30 000	-	-	0.25	2400
	VSB	45 000	-	-	0.2	2400
Steel Bar	VSB	205 800	-	-	0.3	7800
Ballast	VB/ VBZT1	200	-	-	0.35	1700
Sub-ballast	VB	180	-	-	0.35	2135
Ballast mat	VBZT1	-	-	0.0525	0.25	900
Fibrous Concrete	VSB	34 000	-	-	0.2	2400
CSL	VSB	38 000	-	-	0.2	2400
HBL	VBZT1/ VSB	23 000	-	-	0.25	2000
Platform	VB/ VBZT1/ VSB	100	-	-	0.3	1800

[2] Dynamic stiffness

All elements were modeled as 20 nodes hexahedral elements (SOLID95), with the exception of the steel bar from the bi-block sleeper that was modeled as a three-dimensional beam (BEAM4).
Based on the study and sensitivity analysis to the domain of the railway model and through the iterative process associated, a model length of 12 m (21 sleepers with 60 cm spacing) is adopted. The transversal domain has an extension of 7.5 m and platform depth is 4 m.

3.3. Model validation

To enhance the confidence in the developed models and use them as a tool to evaluate the behavior of different railway types, they were validated with experimental results. For each model (VB, VBZT1 and VSB) three types of model variants were applied.

The 1st is of material nature, wherein the elements with mechanical variability, such as ballast (VB and VBZT1), sub-ballast (VB) and the platform (VB, VBZT1, and VSB) were increased by 25% in stiffness.

The 2nd variant was the appliance of several loads, a static (EMW wagon) and two dynamic loads (TGV Réseau static load amplified according to the formulation of Eisenmann and Prud 'Homme). Finally the 3rd variant includes changes in models, in order to evaluate the influence of contact elements and how they influence the vertical stress diagrams of the models, variants were developed with contact elements. The contact elements adopted are TARGET170 and CONTACT174, both surface contact elements with 8 nodes. The TARGET170 models the target surface, which is associated with a deformable contact surface (CONTACT174) which penetrates the target.

The variants of the models evaluated are outlined in Table 3.2. The contact type is frictionless (perfect sliding) without separation in the orthogonal direction to the contact and target surfaces.

Table 3.2: Model variants with contact elements

		Contact element interface		
Model	**Variant**	**Sleeper/ Ballast (CSL)**	**Ballast (CSL) / Sub-ballast (HBL)**	**Sub-ballast (HBL) / Plat.**
VB/ VBZT1	**S/C**	×	×	×
	T	✓	×	×
	TBS/ TBH	✓	✓	✓
VSB	**S/C**	×	×	×
	CH	×	✓	✓

The models are validated by experimental trials conducted by SNCF, especially with a rail and sleeper displacement range that were treated with an appropriate statistical model to validate the vertical flexibility of the tracks.

It was also used another experimental campaign in Spain in a slab track test section between Las Palmas and Castellon Oropesa de Mar in Valencia-Tarragona line where was assessed a study of track parameters as vertical compressive stresses in the multilayer system, rail displacement, reinforcement stress and strain among others.
To complement the validation process, two theoretical approaches were used, with respect

to vertical compressive stresses through Burmister (two elastic layers) and Jones & Piatte (3 elastic layers) charts. To validate the bending moments calculated by the VSB model, the Ray & Pickett influence chart based on Westergaard's rigid pavement theory [14] was applied.

According to the results from the validation process performed, the best fitting model variants are VB T, VBZT1 T and VSB CH. The developed models can be observed in Figure 3.3.

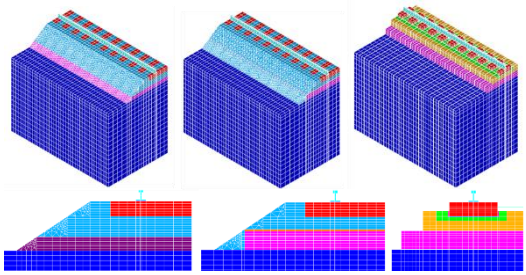

Figure 3.3: VB (left), VBZT1 (center) and VSB (right) models

4. Structural behavior of slab track

After validation of the models described above, the required conditions are met in order to calculate the structural response of a slab track and its comparison with the ballasted track.

4.1. Comparison between slab track and ballasted track

The ballasted track and the slab track present notable differences in their main components, so relevant differences are expected in the structural behavior when requested. The load model applied was a single axle load of 20 tons.

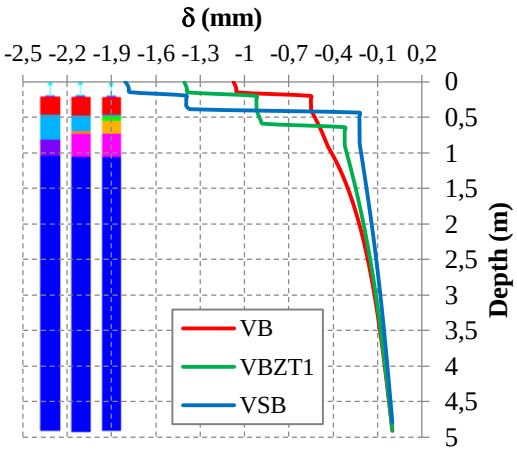

Figure 4.1: Vertical displacements in depth for VB, VBZT1 and VSB

Table 4.1: Rail displacements and track stiffness

Model	δ (mm)	K_p (kN/mm)
VB	-1.15	85.1
VBZT1	-1.51	65.1
VSB	-1.80	52.1

The displacements obtained through numerical modeling show that, due to the low stiffness of the USP, the slab track is the most flexible track, presenting more than 80% of the vertical displacement due to the elastic system. It can be seen in Figure 4.1 that there is a tendency to ensure vertical flexibility through the elastic system gradually towards VB-VSB, in an attempt to replace the elasticity of the ballast and sub-ballast layer for intermediate levels.

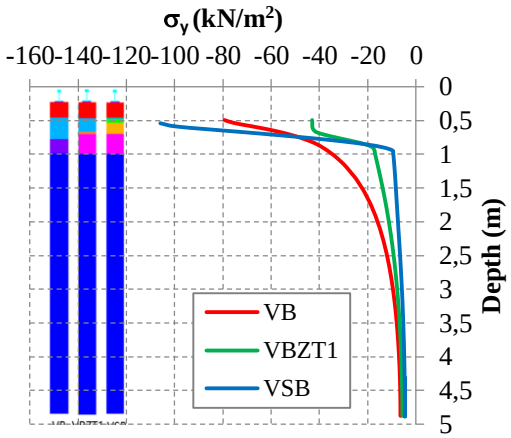

Figure 4.2: Vertical compressive stress in depth for VB, VBZT1 and VSB

Regarding the load distribution on the superstructure, as expected, the slab track has a vertical stress concentration underneath the CSL due its large stiffness, which results also in rapid stress mitigation for the platform. The VBZT1 solution presents the best performance in the distribution of the load under the sleeper due to the joint action of ballast mat (prevents stress concentration on the HBL) and HBL (rapidly degrades the load). This stress reduction under the sleeper reaches 60% compared to the slab tracks and 46% compared to traditional ballasted solution.

The most prominent parameter of the slab track solution is the vertical compressive stress on top of the platform. By direct observation of Figure 4.2, it is seen a 77% reduction of the vertical stress on the platform compared with the current ballasted solution. This reduction is mainly due to the HBL stiffness that highlights its important role to ensure the durability of the entire railway infrastructure.

4.2. Slab track design optimization

4.2.1. Elastic system

The elastic system on slab tracks has a great importance for the track vertical stiffness. In the case of Stedef[TM] solution, the railpad and the USP are responsible for 23% and 63% of the vertical displacement of the track, which shows the great influence of this type of structural element, particularly the USP.

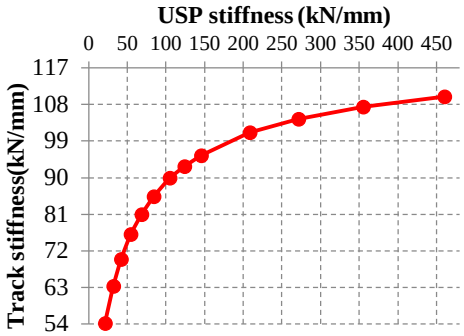

Figure 4.3: Correlation between USP and track stiffness

The influence of USP vertical flexibility shows quite remarkable results obtained in the model-variants (Figure 4.3), in which is observed a strong correlation between the USP stiffness and the vertical track stiffness until 60 kN/mm. It is noted that in the absence of the USP, the track vertical stiffness tends asymptotically to 110 kN/mm, while adopting USP stiffness around 50 to 60 kN / mm, a current track stiffness around 70 to 80 kN/mm can be obtained.

4.2.2. Introduction of a sub-ballast layer

There are some railway administrations that implement sub-ballast layers under the HBL which originates lower vertical stress on the platform, resulting in a longer life span of the structure. To examine the influence of this element on the stress level on the platform, several models with various sub-ballast layers thicknesses (15, 25 and 35 cm) were performed. The sub-ballast layer has the same properties used in the VB model. model variants were also developed, with bituminous sub-ballast with current thicknesses used in this kind of solution with 10, 12 and 14 cm and modulus of elasticity of 6000 MPa and 9000 MPa ($\upsilon = 0.25$) .

As it would be expected, the bituminous sub-ballast layers can achieve significant reductions of vertical stress on the platform, and both solutions in a nearly linear decrease. This almost linear degradation of vertical stresses on the platform it is due to the high stiffness of HBL, which by itself provokes a strong reduction in the vertical stress.

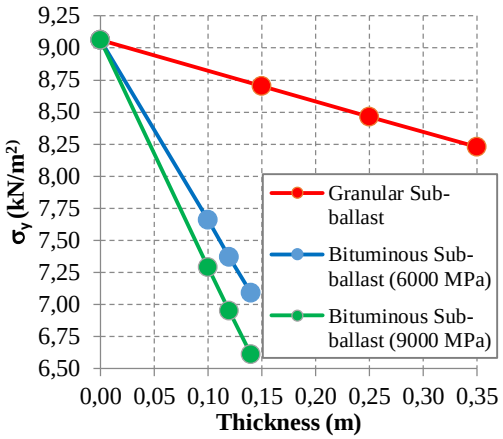

Figure 4.4: Influence in platform vertical stress through the introduction of a sub-ballast layer

The results indicate that a granular sub-ballast layer has a capacity for reducing stress at the top of the platform per cm of 13.6% compared to the 9000 MPa layer.

4.2.3. Geometry of the CSL and HBL

CSL and HBL are the main elements of the slab track superstructure and responsible for the greatest fluctuations of vertical stress between intermediate levels in behalf to its high stiffness. The change in geometry of CSL and HBL will be summarized in thickness variation of 10 and 20 cm for CSL and 20 and 35 cm for the HBL, because a slight reduction in their geometry results in relevant economic gains in initial investment. The results are shown in Table 4.2:

Table 4.2: Influence of CSL and HBL thickness vertical stress

	VSB	C 10	C 20	H 20	H 35
$\sigma_{y\ CSL/HBL}$ (kN/m²)	58.7 (-)	74.0 (26%)	47.0 (-20%)	53.9 (-10%)	61.4 (5%)
$\sigma_{y\ HBL/Plat.}$ (kN/m²)	9.06 (-)	9.4 (4%)	7.8 (-14%)	10.0 (11%)	7.6 (-16%)

As presumed, the CSL has greater influence on the vertical stress at CSL/HBL interface and HBL in HBL/Platform interface. The HBL thickness reduction may be reasonable, since the reduced bending stiffness of the track is not significantly affected (bending moments suffer very low percentage

deviations) and the additional vertical stress on the platform is only slightly greater (≈ 11%), being far from dangerous fatigue limits of the soil.

4.2.4. Introduction of a CAM Layer

Currently, there are types of ballastless tracks, namely the prefabricated Japanese and German solutions (Shinkansen™ and Bögl™), that introduce a cement asphalt mortar (CAM) since it is a relatively inexpensive material and has many advantages in vibration and elasticity behavior improvement.

The CAM thickness varies between 40 and 100 mm, and has a stiffness around 1.25 N/m^3, that will be evaluated by three variants of the original VSB model with a CAM layer in CSL /HBL interface with 40, 70 and 100 mm.

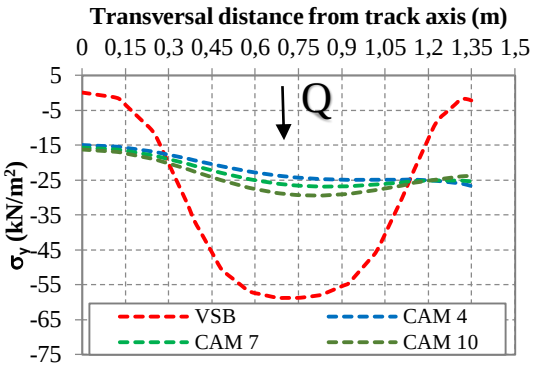

Figure 4.5: Influence of the CAM layer introduction in the CSL/ HBL interface stress diagram

As shown in Figure 4.5, the inclusion of a CAM layer has a strong influence on the degradation of vertical stress verifying significant reductions between CSL/HBL interfaces that exceeded 50%.

4.3. Comparison with other slab track systems

Amongst the main types of slab tracks currently used for high-speed lines around the globe are the system presently studied (Stedef™), the solution with embedded sleepers Rheda 2000™ and the prefabricated solution Bögl™. The modeling of the respective types will be made analogously to the VSB model (Stedef™) with elastic domain and introduction of contact elements between CSL /HBL and HBL/Platform with the usual geometrical dimensions set out in Figure 4.6.

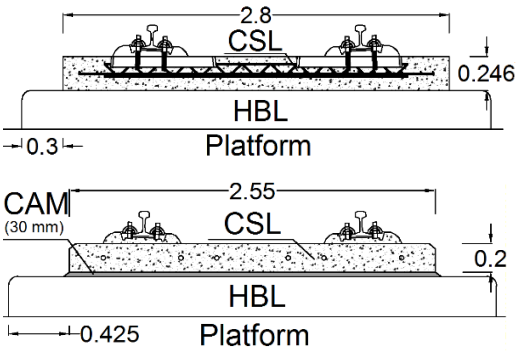

Figure 4.6: Schematic representation of Rheda 2000™ (above) and Bögl™ (below) systems (units in m)

It should be noted that usually the thickness and mechanical properties of HBL are different accordingly to the system used, however for the purpose of comparison between different slab track systems, the same thickness (281 mm) was used. The mechanical properties of the respective elements are described in Table 5.11.

Table 4.3 Rheda 2000™ and Bögl™ properties

Element	Rheda 2000™	Bög™
Rail	E = 205.8 GPa; υ=0.3	
Railpad	Kp=28 kN/mm υ=0.25)	
Sleeper	E = 49 GPa; υ=0.25	-
Steel bar	E = 205.8 GPa; υ=0.3	-
CSL	E = 38 GPa; υ=0.2	
CAM	-	K_{CAM}=1.25 N/mm^3; υ=0.25
HBL	E = 23 GPa; υ=0.25	
Platform	E = 100 Mpa; υ=0.3	

An important aspect to mention is that the model does not include the plate joint of the Bögl™ system, so the hypothesis that the bolted connection between plates is stiff enough to transmit the entire bending moment and shear force resisted by the CSL was adopted. The models are illustrated below:

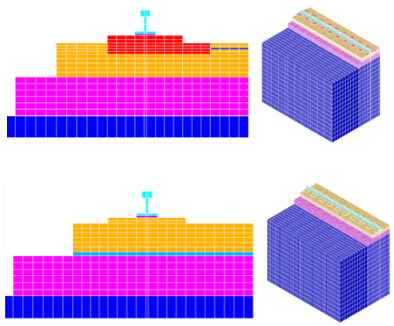

Figure 4.7: Rheda 2000™ (above) and Bögl™ (below) FEM

The three types are very similar in the participation of the elastic system in the vertical flexibility of the track with percentages around 80%, being slightly higher in the Stedef™ case. The extra elasticity provided by the CAM in Bögl™ system only contributes 1.9% for the vertical displacement.

Table 4.4: Rail displacements and track stiffness of different slab track systems

Model	δ (mm)	K_p (kN/mm)
Stedef™	-1.81	54.2
Rheda 2000™	-1.62	60.6
Bögl™	-1.69	57.9

The Bögl™ system is the slab track solution with the lowest vertical stress between CSL/HBL, with reductions of 32.2% compared to Stedef™ system and 44.6% compared to Rheda 2000™ system. This is a result of the extra elasticity provided by the CAM layer proven previously in the design optimization of the Stedef™ system. However, it is important to note that the maximum stress is not on the alignment of the rail. This level of elasticity conferred by the CAM allows the CSL to have a lower flexural rotation than HBL. Thus, the maximum stress is observed near the edges of CSL. It should be pointed that the Stedef™ solution presents the lowest platform stress with reductions of 38.9% compared to the Rheda 2000™ and 45.0% in the Bögl™ system (see Table 4.5).

Table 4.5: Vertical stress comparison of the different slab track systems

	Stedef™	Rheda 2000™	Bögl™
σ_y CSL/HBL	58.7	71.8	39.8
σ_y HBL/ Plat.	9.1	14.8	16.5

Regarding the bending moment acting on the CSL, the Bögl™ system is the slab track model that shows higher bending moments mainly due to very concentrated load (no sleepers) and also by the elastic sub-base provided by the CAM.

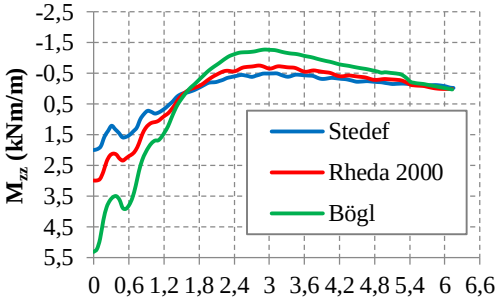

Figure 4.8: Bending moments

4.4. Structural response to platform stiffness variations

The existing literature suggests that the CSL has enough flexural stiffness to uniform some platform irregularities becoming a small overpass on these platform stiffness variations.

Taking this into account, the structural response shall be assessed, in terms of displacement, axial stresses and bending moments of the three types of slab tracks previously described as a consequence of the platform stiffness variations, summarized in two situations illustrated in Figure 4.9.

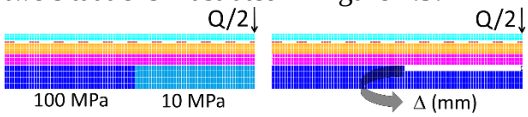

Figure 4.9: Platform stiffness variations

•**Scenario 1**: A section affecting 9 sleepers (≈ 6 m) with a foundation soil with modulus of elasticity 10 times lower than the normal;

•**Scenario 2**: A platform differential settlement affecting 9 sleepers (≈ 6 m), with a 2.5 and 5 mm displacement (Δ);

The main differences in the developed models are: (i) the contact elements used and (ii) the nonlinear concrete behavior.

Regarding the contact elements, the main alteration is the change of the contact algorithm category from no separation (perfect sliding) to standard contact (it can be detached orthogonally from target surfaces) in areas of greater flexibility so that, for example, the weight of the HBL would not be supported by the CSL, which does not actually happen. In order to evaluate the brittle behavior of the concrete a 8 node hexahedral element SOLID65 was used for the CSL and SOLID45 for the remaining elements.

The SOLID65 element requires linear and multilinear material properties. The multilinear materials properties use the Von Mises yield criterion and the William and Warnke model (1974) for brittle concrete behavior are presented in Table 4.6.

Table 4.6: William and Warnke concrete proprieties

Parameter	Value
Open crack shear ratio (β_t)	0.4
Closed crack shear ratio (β_c)	0.8
Uniaxial cracking stress (f_{ctm})	3.2 MPa
Uniaxial crushing stress (f_{cm})	43 MPa

The longitudinal reinforcement is modeled through an ANSYS™ software option that allows to select some elements and reinforce them with a steel rod section with the desired direction. The material used for the reinforcement model was a bilinear kinematic hardening model that requires the yield stress of the S500 and a hardening modulus (≈ 0.01 E_s).

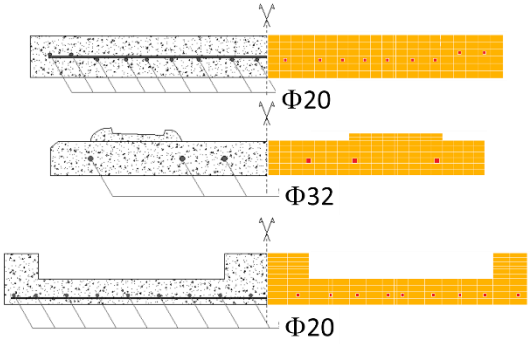

Figure 4.10: Reinforcement schematic representation for the Rheda 2000™ (above), Bögl™ (center) and Stedef™ (below)

The algorithm used to update the stiffness matrix is the Newton-Raphson algorithm with a displacement convergence criterion with a tolerance of 0.05 mm.

For scenario 1, although the CSL does not reach the tensile yield stress of the concrete, an axial stress increase about 3 times it's observed when compared with the reference situation. The bending moments are slightly increased up to 2.5 times more than the reference situation. In a structural point of view, the railway structure presents no problems with the bearing capacity, however the rail displacements almost double, which could cause significant maintenance problems

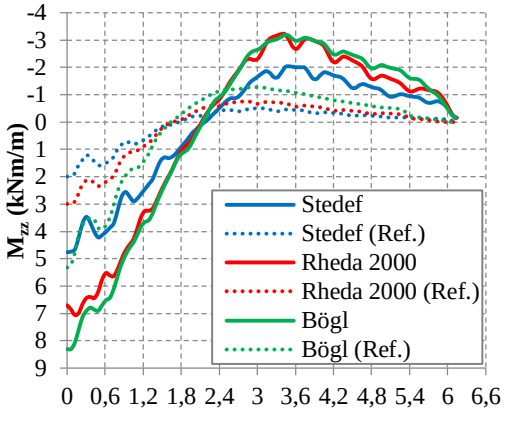

Figure 4.11: Bending moments of scenario 1

The 2nd scenario (occurrence of a platform differential settlement) was divided in 2 situations. As in the first situation, a differential settlement of 2.5 mm along 9 sleepers with a centered 10 ton wheel load, does not cause cracking. Unlike scenario 1, this change in the platform stiffness is subject to a sudden contact between CSL and HBL which can cause crushing of concrete and possible fatigue after millions of load cycles.

Given the observed bending moments, the important aspect to mention is the significant increase of the bending moment in the Bögl™ system (≈ 4 times more than the reference situation) primarily due to the level of elasticity conferred by the CAM layer, that allows excessive deformation of the slab.

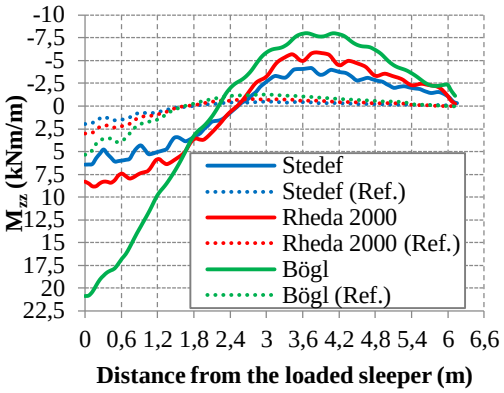

Figure 4.12: Bending moments of scenario 2 (Δ=2.5 mm)

For the case of a platform differential settlement of 5 mm, the Bögl™ and Rheda 2000™ solutions present enough flexibility to allow the contact with the HBL, and all systems exhibit CSL cracking. Through Figure 4.13 it can be seen that the first crack opening at CSL comes around 60% and 75% of the train load (10 tons/wheel), for displacements of the CSL bottom around 3 and 3.5 mm

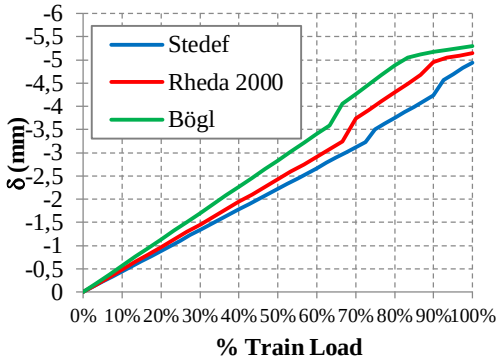

Figure 4.13: CSL vertical displacement for scenario 2 (Δ=2.5 mm)

The Stedef™ slab track is the system which shows better performance, where cracks begin to appear only about 73% of the train

load. The Stedef™ system loses about 8.6% and 2.5% in the vertical stiffness of the first and second crack openings respectively. Bögl™ system loses 5% and Rheda 2000™ system loses 15.7% of its vertical stiffness in the first crack opening.

Despite all systems exhibiting cracking in their CSL, the reinforcement stress is relatively low with 97.2 MPa 76.3 MPa and 39.2 MPa for Stedef™, Rheda 2000™ and Bögl™ systems in the scenario 2. This main difference in reinforcement stress is due to its position in the slab. The Rheda 2000™ and Bögl™ systems place the reinforcement near the neutral axis of the slab (for cracking control induced by temperature variations); in contrast, Stedef™ slab track shows larger reinforcement stress because of their larger eccentricity. Through an indirect calculation and simple approach suggested by EN1992-1 [15] , the maximum crack width for all three systems should be no more than 0.1 mm.

According to the Japanese slab track maintenance recommendations, the required limits are: (i) Class A ($w_k \geq 0.2$ mm) (ii) B (0.2 mm $\geq w_k \geq$0.1 mm) and (iii) C (0.1 mm $\geq w_k \geq$ 0.05 mm) representing respectively the need for quick repair, maintenance operation preparation, scheduling and register in standing book [16]. In German slab track recommendations, the crack width criteria are simplified to a maximum limit of $w_k \leq 0.5$ mm [17]. Along with the results previously obtained, it's not expected major maintenance needs in the slab by the occurrence of the platform longitudinal stiffness variations in a static analysis.

5. Conclusions and further developments

This paper presents the study of a numerical calculation of the static behavior of slab tracks through several three-dimensional finite element models. The main contribution is the development of a numerical tool, properly validated through experimental campaigns and theoretical formulations, that assists decision making and design optimization of slab tracks construction. It is important to mention that all the results and conclusions reached are carried out according to the particular case study and parameters used in the numerical modeling. Regarding the **design optimization** of a slab track, the main conclusions are:

- A USP stiffness around 50 to 60 kN/mm leads to current track stiffness about 70 to 80 kN/mm.
- The introduction of a granular sub-ballast layer reduces the vertical stress on the platform in 4 to 9%. If a bituminous sub-ballast is chosen, the stress reduction can reach 27%.
- The reduction of the HBL thickness from 28 cm to 20 cm only increases the platform stress by 10%, which is still much lower than the observed in the ballasted solution.
- The implementation of a CAM layer gives an extra level of elasticity with significant contribution in stress reductions in the CSL/ HBL interface that exceeds 50%, associated with the advantages of vibratory behavior.

Concerning the **comparison with other slab tracks** currently used in high-speed lines (Stedef™, Rheda 2000™ and Bögl™), the principal evaluations are:

- All systems have very similar vertical stiffness (≈ 60 kN/mm).
- The Stedef™ system exhibits a better degradation of vertical stresses on the platform with a 40% reduction compared with the remaining solutions reviewed.
- All the systems evaluated show a bending moment neutral point about three sleepers away from the loaded sleeper (≈ 1.8 m).

Towards the **platform longitudinal stiffness variations**, with an influence length around 6 m (9 sleepers) the key aspects are:

- For a reduction of the modulus of elasticity of the platform (100 MPa to 10 MPa) or a differential settlement of 2.5 mm, there are no signs of CSL yielding. The increase of bending moment absorbed by CSL is about 3-4 times than the reference situation.
- For a 5 mm differential settlement, there is cracking of the CSL although the reinforcement stress is low (<100 MPa), which, according to the crack width indirect calculations suggested by EN1992-2, results in crack openings probably less than 0.1 mm.

With the advancement of computational power, it is possible to apply more complex analysis for the purpose of the slab track design, the principal **guidelines for future research** are:

- Incorporation of a non-linear behavior for granular materials, HBL and railpad /USP in order to calculate the static response with more detail.
- Development of three-dimensional models for dynamic analysis to estimate accelerations on the track and wheel/rail contact interaction; Study of the slab track response to initial defects in the track.

Other future contributions to continue the work in order to optimize the design of the slab track and life cycle cost reduction are:

- Study of the dynamic behavior of the track and for very high speeds (>350 km/h).
- Study of new reinforcements configurations for cracking control and cracking evolution from the point of view of the joint action of the train load, temperature and differential settlements modeled by their occurrence probability.
- Research on the fatigue of CSL and HBL caused by the joint action of the train loading, temperature and differential settlements for the purpose of evaluating their real life spans.

Acknowledgements

The author would like to thank Dr. Patricia Ferreira (supervisor), whose knowledge and experience share was very important for this final result.

A special thanks to Dr. Paulo Teixeira and Eng. Tiago Ferreira for their collaboration and assistance to this work.

6. References

[1] **Teixeira, P. F. (2003)**, "Contribución a la reducción de los costes de mantenimiento de las vias de alta velocidad mediante la optimización de su rigidez vertical"., Tesis Doctoral. Barcelona: UPC - Universitat Politécnica de Catalunya.

[2] **Areias, A. (2007)**, "Dimensionamento de plataformas ferroviárias de alta velocidade com camadas granulares e betuminosas mediante a utilização de modelos elasto-plásticos por elements finitos", Lisboa: Tese de Mestrado. Instituto Superior Técnico.

[3] **Ferreira, T. M. and Teixeira, P. F. (2012)**, "Rail Track Performance with Different Subballast Solutions: Traffic and Environmental Effects on Subgrade Service Life," *Journal of Transportation Engineering* , vol. 138, pp. 1541-1550.

[4] **Markine, V. L. Man, A. P de, and Esveld, C. (2000)**, "Optimization of an embedded rail structure using a numerical technique," *Delf University of Technology, HERON*, vol. 45, nº 1, pp. 63-74.

[5] **Blanco-Lorenzo, J. Santamaria, J., Vadillo, E.G. and Oyarzabal, O. (2011)**, "Dynamic comparison of different types of slab tracks and ballasted track using a flexible track model," *Proc. ImechE Part F: Journal of Rail and Rapid Transit*, vol. 225, pp. 574-592.

[6] **Vale, C., Ribeiro, N., Calçada R. and Delgado R.. (2011)**, "Dynamics of a Precast System for High-Speed Railway Tracks," in *Third ECCOMAS Thematic Conference on Computational Methods in Structural Dynamics and Earthquake Engineering*, Corfu, Grécia.

[7] **Poveda, E. Yu, R. C., Lancha, J. C and Ruiz, G. (2012)**, "Finite element analysis on the fatigue damage under compression of a concrete slab track," in *VIII Intenational Conference on Fracture Mechanics of Concrete and Concrete Structures*, Toledo, Espanha.

[8] **ANSYS Inc.**, *Documentation for Release 12.1.*

[9] **Morais, J., (2008)**, "Impacto das variações de rigidez vertical da via na degradação das linhas férreas e alta velocidade", Lisboa: Tese de Mestrado. Instituto Superior Técnico.

[10] **Ministerio de Fomento, (1999)**, "Recomendaciones para el proyecto de plataformas ferroviarias", Secretaria de Estado de Infrastructuras y Transportes, Área de Infraestrucutura Ferroviaria. Series Normativas.

[11] **SNCF, (2004)**, "Zone test VSB", LGV Est européenne - Ligne nouvelle de Vaires À Vendenheim: Direction des Superstructures Ferroviares - Grand Projects. Document confidentiel, 2004.

[12] **SNCF, (2012)**, "Mesures d'accélérations et de nivellement sur zone de transition," LGV Est-Européenne - VSB km 18+600 et km 20+200. Document confidentiel.

[13] **Y. Huang, (1993)**, "Pavement analysis and design", Prentice Hall Inc.

[14] **CEN, Comité Européen de Normalisation, (2004)**, "Eurocode 2: Design of concrete structures - Part 1-1: General rules and rules for buildings, EN 1992-1-1".

[15] **Xie, Y. *et. al.* (2009)**, "Concrete Crack of Ballastless Track Structure and its Repair," *IJR International Journal of Railway*,Vol.2, No. 1, pp. pp. 30-36.

[16] **Lichtberger, B. (2005)**, "Track Compendium", First Edition ed., Eurorail Press.